

Quantum Repeaters with Photon Pair Sources and Multi-Mode Memories

Christoph Simon, Hugues de Riedmatten, Mikael Afzelius, Nicolas Sangouard, Hugo Zbinden, and Nicolas Gisin
Group of Applied Physics, University of Geneva, Switzerland
 (Dated: October 29, 2018)

We propose a quantum repeater protocol which builds on the well-known DLCZ protocol [L.M. Duan, M.D. Lukin, J.I. Cirac, and P. Zoller, *Nature* **414**, 413 (2001)], but which uses photon pair sources in combination with memories that allow to store a large number of temporal modes. We suggest to realize such multi-mode memories based on the principle of photon echo, using solids doped with rare-earth ions. The use of multi-mode memories promises a speedup in entanglement generation by several orders of magnitude and a significant reduction in stability requirements compared to the DLCZ protocol.

The distribution of entanglement over long distances is an important challenge in quantum information. It would extend the range for tests of Bell's inequalities, quantum key distribution and quantum networks. The direct distribution of entangled states is limited by transmission losses. For example, 1000 km of standard telecommunications optical fiber have a transmission of order 10^{-20} . To distribute entanglement over such distances, quantum repeaters [1] are likely to be required. Implementations of quantum repeaters have been proposed in various systems, including atomic ensembles [2], single atoms [3], NV centers [4] and quantum dots [5, 6]. A basic element of all protocols is the creation of entanglement between neighboring nodes A and B , typically conditional on the outcome of a measurement, e.g. the detection of one or more photons at a station between two nodes. In order to profit from a nested repeater protocol [1], the entanglement connection operations creating entanglement between non-neighboring nodes can only be performed once one knows the relevant measurement outcomes. This requires a communication time of order L_0/c , where L_0 is the distance between A and B . Conventional repeater protocols are limited to a single entanglement generation attempt per elementary link per time interval L_0/c . Here we propose to overcome this limitation using a scheme that combines photon pair sources and memories that can store a large number of distinguishable temporal modes. We also show that such memories could be realized based on the principle of photon echo, using solids doped with rare-earth ions.

Our scheme is inspired by the DLCZ protocol [2], which uses Raman transitions in atomic ensembles that lead to non-classical correlations between atomic excitations and emitted photons [7]. The basic procedure for entanglement creation between two remote locations A and B in our protocol requires one memory and one source of photon pairs at each location, denoted $M_{A(B)}$ and $S_{A(B)}$ respectively. The two sources are coherently excited such that each has a small probability $p/2$ of creating a pair, corresponding to a state

$$\left(1 + \sqrt{\frac{p}{2}}(e^{i\phi_A} a^\dagger a'^\dagger + e^{i\phi_B} b^\dagger b'^\dagger) + O(p)\right) |0\rangle. \quad (1)$$

Here a and a' (b and b') are the two modes corresponding to S_A (S_B), ϕ_A (ϕ_B) is the phase of the pump laser at location A (B), and $|0\rangle$ is the vacuum state. The $O(p)$ term introduces errors in the protocol, leading to the requirement that p has to

be kept small, cf. below. The photons in modes a and b are stored in the local memories M_A and M_B . The modes a' and b' are coupled into fibers and combined on a beam splitter at a station between A and B . The modes after the beam splitter are $\tilde{a} = \frac{1}{\sqrt{2}}(a'e^{-i\chi_A} + b'e^{-i\chi_B})$, $\tilde{b} = \frac{1}{\sqrt{2}}(a'e^{-i\chi_A} - b'e^{-i\chi_B})$, where $\chi_{A,B}$ are the phases acquired by the photons on their way to the central station. Detection of a single photon in \tilde{a} , for example, creates a state $|\Phi_{AB}\rangle = \frac{1}{\sqrt{2}}(a^\dagger e^{i\theta_A} + b^\dagger e^{i\theta_B})|0\rangle$ (neglecting $O(p)$ corrections), with $\theta_{A(B)} = \phi_{A(B)} + \chi_{A(B)}$, where a and b are now stored in the memories. This can be rewritten as an entangled state of the two memories,

$$|\Phi_{AB}\rangle = \frac{1}{\sqrt{2}}(|1\rangle_A |0\rangle_B + e^{i\theta_{AB}} |0\rangle_A |1\rangle_B), \quad (2)$$

where $|0\rangle_{A(B)}$ denotes the empty state of $M_{A(B)}$, $|1\rangle_{A(B)}$ denotes the state storing a single photon, and $\theta_{AB} = \theta_B - \theta_A$.

This entanglement can be extended via entanglement swapping as in Ref. [2]. Starting from entangled states $|\Phi_{AB}\rangle = \frac{1}{\sqrt{2}}(a^\dagger + e^{i\theta_{AB}} b^\dagger)|0\rangle$ between memories M_A and M_B , and $|\Phi_{CD}\rangle = \frac{1}{\sqrt{2}}(c^\dagger + e^{i\theta_{CD}} d^\dagger)|0\rangle$ between M_C and M_D , one can create an entangled state between M_A and M_D by converting the memory excitations of M_B and M_C back into propagating photonic modes and combining these modes on a beam splitter. Detection of a single photon after the beam splitter, e.g. in the mode $\frac{1}{\sqrt{2}}(b + c)$, will create an entangled state of the same type between M_A and M_D , namely $\frac{1}{\sqrt{2}}(a^\dagger + e^{i(\theta_{AB} + \theta_{CD})} d^\dagger)|0\rangle$. In this way it is possible to establish entanglement between more distant memories, which can be used for quantum communication as follows [2].

Suppose that location A (Z) contains a pair of memories M_{A1} and M_{A2} (M_{Z1} and M_{Z2}), and that entanglement has been established between M_{A1} and M_{Z1} , and between M_{A2} and M_{Z2} , i.e. that we have a state $\frac{1}{2}(a_1^\dagger + e^{i\theta_1} z_1^\dagger)(a_2^\dagger + e^{i\theta_2} z_2^\dagger)|0\rangle$. The projection of this state onto the subspace with one memory excitation in each location is

$$|\Psi_{AZ}\rangle = \frac{1}{\sqrt{2}}(a_1^\dagger z_2^\dagger + e^{i(\theta_2 - \theta_1)} a_2^\dagger z_1^\dagger)|0\rangle, \quad (3)$$

which is analogous to conventional polarization or time-bin entangled states. The required projection can be performed post-selectively by converting the memory excitations back into photons and counting the number of photons in each lo-

cation. Measurements in arbitrary bases are possible by combining modes a_1 and a_2 (and also z_1 and z_2) on beam splitters with appropriate transmission coefficients and phases.

The repeater scheme described above is attractive because it requires only pair sources, photon memories and linear optical components. The reliance on a single detection for the elementary entanglement creation makes it less sensitive to fiber losses than schemes based on coincident two-photon detections [8]. The price to pay is the requirement of phase stability, cf. below.

The time required for a successful creation of an entangled state of the form Eq. (3) is given by

$$T_{tot} = \frac{L_0}{c} \frac{1}{P_0 P_1 \dots P_n P_{pr}} \left(\frac{3}{2}\right)^{n+1}. \quad (4)$$

Here $L_0 = L/2^n$, where L is the total distance and n is the nesting level of the repeater. The basic clock interval is L_0/c , the time required for the photons to propagate from the sources to the central station and for the information about the result to propagate back to the memories. The success probability for entanglement creation for a single elementary link is denoted by P_0 ; P_i is the success probability for entanglement swapping at the i -th level, and P_{pr} is the probability for a successful projection onto the state Eq. (3). The probabilities P_i and P_{pr} , which are calculated in Ref. [2], depend on the detection and memory efficiencies. The factors of $\frac{3}{2}$ arise because entanglement has to be generated for two links before every entanglement connection. If the average waiting time for entanglement generation for one link is T , there will be a success for one of the two after $\frac{T}{2}$; then one has to wait a time T on average for the second one, giving a total of $\frac{3T}{2}$.

For a single creation of the state Eq. (1) per interval L_0/c the success probability P_0 is equal to $P_0^{(1)} = p\eta L_0 \eta_D$, where η_D is the photon detection efficiency and $\eta_{L_0} = e^{-L_0/(2L_{att})}$, with L_{att} the fiber attenuation length; $P_0^{(1)}$ is typically very small. However, photon pair sources can have repetition rates much higher than c/L_0 , which is of order 1 kHz for L_0 of order 200 km. This leads one to ask whether it is possible to make several entanglement creation attempts per interval L_0/c . The source S_A then produces pairs of photons in correlated pairs of temporal modes (“time bins”) a_k, a'_k , with $k = 1, \dots, N$. All the modes a_k are stored in the memory M_A , and analogously for S_B and M_B . If there is a detection behind the central beam splitter for the m -th time bin, for example in the mode $\tilde{a}_m = \frac{1}{\sqrt{2}}(a'_m e^{-i\chi_A} + b'_m e^{-i\chi_B})$, then we know that a state $|\Phi_{AB}^{(m,m)}\rangle = \frac{1}{\sqrt{2}}(a_m^\dagger e^{i\theta_A} + b_m^\dagger e^{i\theta_B})|0\rangle$ is stored in the memories M_A and M_B , cf. Fig. 1(a). Running the same protocol for another pair of sources S_C, S_D and memories M_C, M_D , there may be a detection in the n -th time bin, leading to a state $|\Phi_{CD}^{(n,n)}\rangle = \frac{1}{\sqrt{2}}(c_n^\dagger e^{i\theta_C} + d_n^\dagger e^{i\theta_D})|0\rangle$ being stored in the memories M_C and M_D . One can then perform entanglement swapping by re-converting the memory modes b_m and c_n into photonic modes and combining them on a beam splitter, cf. Fig. 1(b). This leads to an entangled state

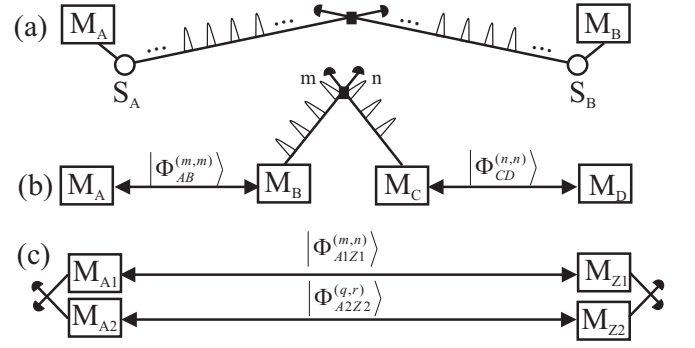


FIG. 1: Quantum repeater scheme using pair sources and multi-mode memories. (a) The sources S_A and S_B can each emit a photon pair into a sequence of time bins. The detection of a single photon behind the beam splitter at the central station projects the memories M_A and M_B into an entangled state Eq. (2). (b) If entangled states have been established between the m -th time bins in M_A and M_B , and between the n -th time-bins in M_C and M_D , an entangled state between the m -th time bin in M_A and the n -th time bin in M_D can be created by re-converting the memory modes into photonic modes and combining the appropriate time-bins on a beam splitter. (c) Useful entanglement can be created between two pairs of distant memories as in Ref. [2]. Again the appropriate time bins have to be combined on beam splitters.

$|\Phi_{AD}^{(m,n)}\rangle = \frac{1}{\sqrt{2}}(a_m^\dagger e^{i(\theta_A+\theta_C)} + d_n^\dagger e^{i(\theta_B+\theta_D)})|0\rangle$ between the m -th mode stored in M_A and the n -th mode stored in M_D . Entanglement of the type Eq. (3) can be created as before, again by combining the appropriate time bins, cf. Fig. 1(c).

The described protocol requires memories that allow to store and retrieve the various temporal modes a_i, b_i etc., preserving their distinguishability. We refer to such memories as *multi-mode memories (MMMs)*. We describe below how MMMs can be realized based on the photon echo principle, which ensures that photons absorbed at different times are emitted at different times. With MMMs, working with N attempts per interval increases the success probability from $P_0^{(1)} = p\eta L_0 \eta_D$ to $P_0^{(N)} = 1 - (1 - P_0^{(1)})^N$, which is approximately equal to $N P_0^{(1)}$ for $N P_0^{(1)} \ll 1$, increasing the overall success rate of the repeater by a factor of N . Our approach based on pair sources and MMMs can be used to speed up other protocols by the same factor, in particular schemes based on coincident two-photon detection [8], because the speedup occurs at the most basic level, that of elementary entanglement generation. There is no obvious equivalent to the use of MMMs as described above within the Raman-transition based approach of Ref. [2], since all stored modes would be retrieved at the same time, when the relevant control beam is turned on. Other forms of multiplexing (spatial, frequency) can be applied in a similar way both to our protocol and the DLCZ protocol [9].

We now discuss how to realize the elements of our proposal in practice. Photon pair sources with the required properties (sufficiently high p , appropriate bandwidth, cf. below) can be realized both with parametric down-conversion [10] and

with atomic ensembles [7, 11]. Several approaches to the realization of photon memories have been proposed and studied experimentally, including EIT [12], off-resonant interactions [13] and photon echo [14]. The echo approach lends itself naturally to the storage of many temporal modes. Storage and retrieval of up to 1760-pulse sequences has been demonstrated [15]. The temporal information is stored in the relative phases of atomic excitations at different frequencies. Photon echoes based on controlled reversible inhomogeneous broadening (CRIB) [16, 17] allow in principle perfect reconstruction of the stored light. The method is well adapted to atomic ensembles in solids, e.g. crystals doped with rare-earth ions. To implement such a memory, one has to prepare a narrow absorption line inside a wide spectral hole, using optical pumping techniques [18]. The line is artificially inhomogeneously broadened, e.g. by applying an electric field gradient. Then the light can be absorbed, e.g. a train of pulses as described above. After the absorption the electric field is turned off, and atoms in the excited state are transferred by a π -pulse to a second low-lying state, e.g. a different hyperfine state. For recall, the population is transferred back to the excited state by a counter-propagating π -pulse, and the electric field is turned back on with the opposite sign, thereby inverting the inhomogeneous broadening. This leads to a time reversal of the absorption. The pulse train is re-emitted in inverted order, with a retrieval efficiency that is not limited by re-absorption [16]. Photons absorbed in different memories at different times can be re-emitted simultaneously (as in Fig. 1) by choosing appropriate times for the sign-flip of the applied electric field.

The achievable memory efficiency is [19]

$$\eta_M(t) = (1 - e^{-\alpha_0 L \gamma_0 / \gamma})^2 \text{sinc}^2(\gamma_0 t), \quad (5)$$

where for simplicity we consider square spectral atomic distributions, both for the initial narrow line and the artificially broadened line. Here $\alpha_0 L$ is the optical depth of the medium before the artificial broadening, γ_0 is the initial spectral distribution width, γ is the width after broadening, and t is the time before transfer to the hyperfine state (neglecting hyperfine decoherence). The above formula is exact for all pulse shapes whose spectral support is completely inside the square atomic distribution. Otherwise there are additional losses due to spectral truncation of the pulse. The width γ has to be large enough to allow for pulse durations significantly shorter than the interval between pulses Δt , in order to avoid errors due to pulse overlap. For truncated Gaussian pulses choosing $\gamma \Delta t = 6$ is sufficient for such errors to be negligible. On the other hand, γ is required to be smaller than the separation between the hyperfine states used in the memory protocol and whatever state is used for shelving unwanted atoms in the preparation of the initial spectral hole (e.g. another hyperfine state). The initial width γ_0 has to fulfill $\gamma_0 > 2\gamma_h$, where γ_h is the homogeneous linewidth of the relevant transition [20]; γ_0 should be chosen such as to optimize $\bar{\eta}_M$, the average of Eq. (5) over all time-bins, i.e. for t between 0 and $N\Delta t$. One can show that $\bar{\eta}_M$ can be expressed as a function of the two variables $x = \gamma_0 N \Delta t$ and $y = \alpha_0 L / N$. By adjusting γ_0 one can choose, for a given

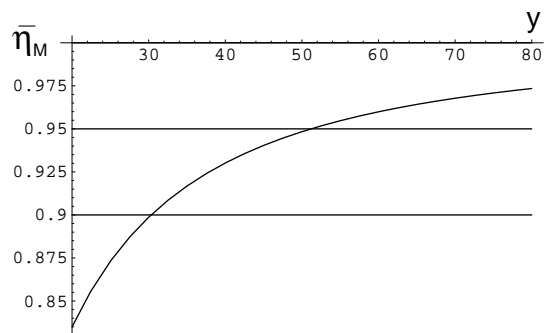


FIG. 2: The maximum achievable average efficiency $\bar{\eta}_M$ as a function of $y = \alpha_0 L / N$. One can see that $\bar{\eta}_M = 0.9$ is obtained for $y = 30$. This implies that storing $N = 100$ time-bins with this average efficiency requires $\alpha_0 L = 3000$, while 1000 time-bins require $\alpha_0 L = 30000$; $\bar{\eta}_M = 0.95$ is obtained for $y = 50$. The required values of $x = \gamma_0 N \Delta t$ are $x = 0.8$ for $\bar{\eta}_M = 0.9$ and $x = 0.6$ for $\bar{\eta}_M = 0.95$.

value of y , the value of x that maximizes $\bar{\eta}_M$. Then $\bar{\eta}_M$ becomes a function of y only, which is plotted in Fig. 2.

The storage has to be phase-preserving, so as to conserve the entanglement for the states of Eqs. (2-3). Decoherence can affect the excited states during the absorption of the pulse train, and the hyperfine ground states during the long-term storage. In rare-earth ions, excited state coherence times ranging from tens of μs to 6 ms [21] and hyperfine coherence times as long as 30 s [22] have been demonstrated. For a recent experimental investigation of phase coherence in photon echo with rare-earth ions see Ref. [23].

We now discuss how to achieve high values for N and $\bar{\eta}_M$ experimentally. Pr:Y₂SiO₅ is a very promising material for initial experiments, since excellent hyperfine coherence [22] and memory efficiencies of order 13 % [17] for macroscopic light pulses have already been demonstrated. The main drawback of Pr is the small hyperfine separation (of order a few MHz), which limits the possible pulse bandwidth and thus N , since by definition $N \leq \frac{L_0}{c\Delta t} = \frac{L_0\gamma}{6c}$. Neodymium and Erbium have hyperfine separations of hundreds of MHz [24, 25]. Nd also has strong absorption, e.g. Nd:YVO₄ with a Nd content of 10 ppm has an absorption coefficient $\alpha_0 = 100/\text{cm}$ [21] at 879 nm. Choosing $\gamma = 300$ MHz (which gives $\Delta t = 6/\gamma = 20$ ns) and $\gamma_0 = 100$ kHz, which is well compatible with $\gamma_h = 10$ kHz as measured for Nd in [21], our above calculations show that e.g. $N = 400$ and $\bar{\eta}_M = 0.9$ would be possible with $\alpha_0 L = 30N = 12000$, which could be achieved with a multi-pass configuration. Erbium-doped materials can combine good optical coherence and large inhomogeneous linewidth, e.g. $\gamma_h = 2$ kHz and $\Gamma_{inh} = 250$ GHz for Er:LiNbO₃ [21], which makes Er a natural candidate for the implementation of frequency multiplexing in addition to temporal multiplexing. The protocol could be run in parallel for a large number of frequency channels. Even taking into account the lower absorption for Er, this might allow one to gain an order of magnitude or more for the overall value of N

compared to our Nd example.

To assess the potential performance of our scheme, consider a distance $L = 1000$ km, and a fiber attenuation of 0.2 dB/km, corresponding to telecom wavelength photons. Note that the wavelengths of the photon propagating in the fiber and of the photon stored in the memory can be different in our scheme. Assume $\bar{\eta}_M=0.9$ and photon-number-resolving detectors with efficiency $\eta_D = 0.9$. Highly efficient number-resolving detectors are being developed [26, 27]. One can show that the optimal nesting level for the repeater protocol for these values is $n = 2$, corresponding to $2^n = 4$ elementary links, which gives $L_0 = 250$ km. Using Eq. (4) and Ref. [2] one can show that the total time for creating a state of the form Eq. (3) using the scheme of Fig. 1 is

$$T_{tot} = \frac{L_0}{c} \frac{18(2-\eta)(4-3\eta)}{Np\eta_{L_0}\eta_D\eta^4}, \quad (6)$$

where $\eta = \bar{\eta}_M\eta_D$ and $\eta_{L_0} = e^{-L_0/(2L_{att})}$, with $L_{att} = 22$ km, and $c = 2 \times 10^8$ m/s in the fiber. One can show by explicit calculation of the errors due to double emissions [28] that the fidelity F of the final entangled state compared to the ideal maximally entangled state for a repeater with $n = 2$ levels is approximately $F = 1 - 56(1 - \eta)p$. If one wants, for example, $F = 0.9$ one therefore has to choose $p = 0.009$, which finally gives $T_{tot} = 3400/N$ s. If one can achieve $\bar{\eta}_M = \eta_D = 0.95$ one finds $T_{tot} = 800/N$ s. High-efficiency MMMs as discussed above could thus reduce T_{tot} for 1000 km to a few seconds (or less with frequency multiplexing).

MMMs can also help to significantly alleviate the stability requirements for the repeater protocol. For simplicity, let us just consider an elementary link (between locations A and B) from our above example, with $L_0 = 250$ km. The entanglement in Eq. (3) depends on the phase difference $\theta_2 - \theta_1$, which can be rewritten as $(\theta_{B_2}(t_2) - \theta_{B_1}(t_1)) - (\theta_{A_2}(t_2) - \theta_{A_1}(t_1))$. Here t_1 (t_2) is the time when the first (second) entangled state of the type of Eq. (2) is created. The phases thus have to remain very stable on the timescale given by the typical value of $t_2 - t_1$ [29]. In the case without MMMs the mean value of $t_2 - t_1$ is $L_0/(cP_0)$, which is of order 10 s for our above example (L_0/c of order 1 ms and P_0 of order 10^{-4}). Over such long timescales, both the phases of the pump lasers and the fiber lengths are expected to fluctuate significantly. Active stabilization would thus definitely be required. With MMMs, for large values of N , P_0 can be made sufficiently large that it becomes realistic to work only with states Eq. (3) where the initial entanglement between A_1 and B_1 and between A_2 and B_2 was created in the same interval L_0/c (the probability for such a double success is P_0^2). For our above example, P_0 can be made of order 10^{-1} for N of order 10^3 . Working only with entangled states from the same interval increases the time T_{tot} by a factor of order $1/P_0$, but it reduces the mean value of $t_2 - t_1$ to of order $N\Delta t$, which is of order 20 μ s for our example. For such short time scales, active stabilization of the laser and fiber phases may not be required.

In conclusion the combination of photon pair sources and

multi-mode memories should allow the realization of a quantum repeater protocol that is much faster and more robust than the protocol of Ref. [2] while retaining its attractive features, in particular the use of linear optical elements and of single photon detections for entanglement generation and swapping.

Acknowledgements. We thank M. Halder, S. Kröll, J. Minář, V. Scarani, and W. Tittel for useful discussions. This work was supported by the EU Integrated Project *Qubit Applications* and by the Swiss NCCR *Quantum Photonics*.

-
- [1] H.-J. Briegel *et al.*, Phys. Rev. Lett. **81**, 5932 (1998).
 - [2] L.-M. Duan *et al.*, Nature **414**, 413 (2001).
 - [3] H. Mabuchi *et al.*, Quant. Inf. Comp. **1**, Special Issue 7 (2001).
 - [4] L. Childress *et al.*, Phys. Rev. Lett. **96**, 070504 (2006)
 - [5] P. van Loock *et al.*, Phys. Rev. Lett. **96**, 240501 (2006).
 - [6] C. Simon *et al.*, Phys. Rev. B **75**, 081302(R) (2007).
 - [7] A. Kuzmich *et al.*, Nature **423**, 731 (2003); C.H. van der Wal *et al.*, Science **301**, 196 (2003); J. Laurat *et al.*, Opt. Express **14**, 6912 (2006).
 - [8] L.M. Duan *et al.*, Quant. Inf. Comp. **4**, 165 (2004).
 - [9] O.A. Collins *et al.*, Phys. Rev. Lett. **98**, 060502 (2007).
 - [10] M. Halder *et al.*, Phys. Rev. A **71**, 042335 (2005); C.E. Kulewicz, F.N.C. Wong, and J.H. Shapiro, Phys. Rev. Lett. **97**, 223601 (2006); M. Halder *et al.*, in preparation.
 - [11] V. Balić *et al.*, Phys. Rev. Lett. **94**, 183601 (2005); J.K. Thompson *et al.*, Science **313**, 74 (2006).
 - [12] M. Fleischhauer and M.D. Lukin, Phys. Rev. Lett. **84**, 5094 (2000); T. Chanelière *et al.*, Nature **438**, 833 (2005); M.A. Eisaman *et al.*, Nature **438**, 837 (2005); A.V. Gorshkov *et al.*, quant-ph/0604037 (2006).
 - [13] B. Julsgaard *et al.*, Nature **432**, 482 (2004).
 - [14] T.W. Mossberg, Opt. Lett. **7**, 77 (1982); S.A. Moiseev and S. Kröll, Phys. Rev. Lett. **87**, 173601 (2001).
 - [15] H. Lin, T. Wang, and T.W. Mossberg, Opt. Lett. **20**, 1658 (1995).
 - [16] M. Nilsson and S. Kröll, Opt. Comm. **247**, 393 (2005); B. Kraus *et al.*, Phys. Rev. A **73**, 020302(R) (2006); A.L. Alexander *et al.*, Phys. Rev. Lett. **96**, 043602 (2006).
 - [17] G. Hétet *et al.*, quant-ph/0612169 (2006).
 - [18] G. J. Pryde, M. J. Sellars, and N. B. Manson Phys. Rev. Lett. **84**, 1152 (2000); M. Nilsson *et al.*, Phys. Rev. B **70**, 214116 (2004).
 - [19] N. Sangouard *et al.*, Phys. Rev. A **75**, 032327 (2007).
 - [20] E.S. Maniloff *et al.*, Chem. Phys. **193**, 173 (1995).
 - [21] Y. Sun *et al.*, J. Lumin. **98**, 281 (2002).
 - [22] E. Fraval, M.J. Sellars, and J.J. Longdell, Phys. Rev. Lett. **95**, 030506 (2005).
 - [23] M.U. Staudt *et al.*, Phys. Rev. Lett. **98**, 113601 (2007)
 - [24] R.M. Macfarlane, R.S. Meltzer, and B.Z. Malkin, Phys. Rev. B **58**, 5692 (1998).
 - [25] O. Guillot-Noël *et al.*, Phys. Rev. B **74**, 214409 (2006).
 - [26] J. Kim *et al.*, Appl. Phys. Lett. **74**, 902 (1999); S. Takeuchi *et al.*, Appl. Phys. Lett. **74**, 1063 (1999).
 - [27] D. Rosenberg *et al.*, Phys. Rev. A **71**, 061803(R) (2005).
 - [28] C. Simon *et al.*, in preparation.
 - [29] Note that it is possible to use the same fibers to connect A_1 and A_2 and respectively B_1 and B_2 to the central station [2].